CHEMISTRY OF MATERIALS
Cite This: Chem. Mater. 2019, 31, 2707 2712
Article
pubs.acs.org/cm

# Scaffold-Induced Diketopyrrolopyrrole Molecular Stacks in a Covalent Organic Framework

Sabrina Rager,[†] Andreas C. Jakowetz,[†] Bappaditya Gole,[‡] Florian Beuerle,[‡] Dana D. Medina,*[,†] and Thomas Bein*[,†]

[†]Department of Chemistry and Center for NanoScience (CeNS), University of Munich (LMU), Butenandtstr. 5 13, 81377 Munich, Germany

[‡]University of Würzburg, Institute of Organic Chemistry and Center for Nanosystems Chemistry (CNC), Am Hubland, 97074 Würzburg, Germany

Supporting Information

ABSTRACT: In recent years, covalent organic frameworks (COFs) have attracted considerable attention due to their crystalline and porous nature, which positions them as intriguing candidates for diverse applications such as catalysis, sensing, or optoelectronics. The incorporation of dyes or semiconducting moieties into a rigid two dimensional COF can offer emergent features such as enhanced light harvesting or charge transport. However, this approach can be challenging when dealing with dye molecules that exhibit a large aromatic backbone, since the steric demand of solubilizing side chains also needs to be integrated into the framework. Here, we report the successful synthesis of DPP2 HHTP COF consisting of diketopyrrolopyrrole (DPP) diboronic acid and hexahydroxytriphenylene (HHTP) building blocks. The well known boronate ester coupling motif guides the formation of a planar and rigid backbone and long range molecular DPP stacks, resulting in a highly crystalline and porous material. DPP2 HHTP COF exhibits excellent optical properties including strong absorption over the visible spectral range, broad emission into the NIR and a singlet lifetime of over 5 ns attributed to the formation of molecular stacks with J type interactions between the DPP subcomponents in the COF. Electrical conductivity measurements of crystalline DPP2 HHTP COF pellets revealed conductivity values of up to $10^{-6}$ S cm$^{-1}$.

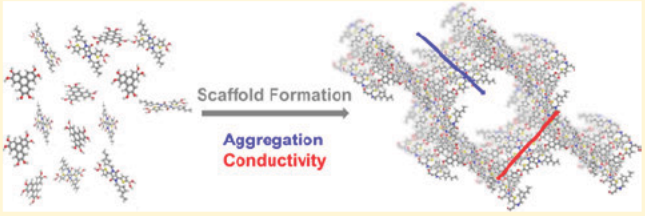


The deterministic synthesis of crystalline porous materials has attracted much interest in recent years.[1,2] Among these, covalent organic frameworks (COFs) offer highly versatile systems due to their tunable linkage chemistry and diverse types of molecular building blocks incorporated into the backbone.[3,4] By molecular design of the building blocks constituting the COFs, structural properties such as the pore geometry, dimensionality, and accessibility can be predicted. In addition, by implementing functional building blocks like photoactive molecules into the framework, physical properties such as broadband light absorption can be encoded, which is of particular importance for optoelectronic and photovoltaic applications.[5−7] Another important operative design tool is the binding motif connecting the building blocks, and fully conjugated or electronically separated systems can be realized depending on the type of cross linking. In the particular case of assembling two dimensional (2D) COFs, defined molecular stacks and thereby the decoupling of electronic properties in different directions can be achieved.[8] One promising synthesis strategy is to harness this type of 2D COF assemblies to construct electroactive macromolecules with overlapping $\pi$ systems featuring desired properties such as long range order and defined host cavities.

COFs featuring electrical conductivity were recently reported,[8] including COF−polymer hybrid systems based on a DAAQ TFP COF film consisting of the electroactive diaminoanthraquinone building block, followed by electro polymerization of 3,4 ethylenedioxythiophene (EDOT) within the pores. The resulting poly(3,4 ethylenedioxythiophene) (PEDOT) infiltrated COF showed enhanced electrical con ductivity.[9] Zhang and co workers reported the synthesis of a conducting tetrathiafulvalene imine based COF that can act as an electron donor. Further doping with iodine improved the conductivity of the bulk material, to reach $1.8 \times 10^{-6}$ S cm$^{-1}$ after two days of doping.[10]

To achieve strong and broadband light absorption, porphyrins and related dyes are prominent building blocks of choice for the construction of COFs. Through the functional design of these photoactive building blocks, 2D[11,12] as well as three dimensional[13] COFs could be established. For example, metalloporphyrins allow for optical band gap tuning in the corresponding COFs.[11,13,14] Moreover, Dichtel et al.[15] and Jiang et al.[16] reported the synthesis of octahydroxyphthalocya nine based COFs by reacting with boronic acid building blocks and demonstrated the generation of photocurrent.[16−18] Another versatile family of dyes is based on the isoindigo

Received: July 9, 2018
Revised: February 5, 2019
Published: February 6, 2019




DOI: 10.1021/acs.chemmater.8b02882
Chem. Mater. 2019, 31, 2707−2712

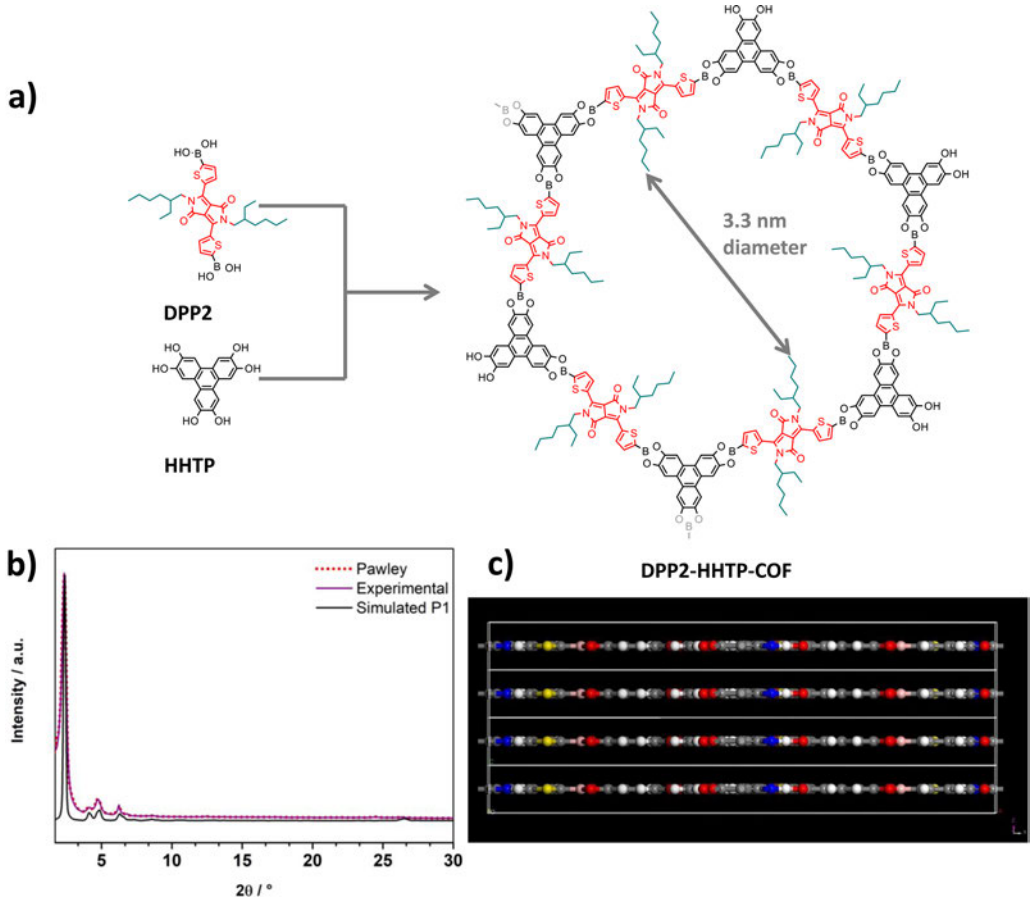


**Figure 1.** (a) Schematic reaction pathway for the synthesis of **DPP2 HHTP COF**. (b) Experimentally obtained powder pattern of **DPP2 HHTP COF** (purple) compared to the calculated diffraction pattern of the eclipsed 2D layer arrangement in the *P*1 space group (black) and Pawley refinement (red). (c) Simulated stacked unit cells for a triclinic crystal system of the space group *P*1 (solubilizing ethylhexyl chains are omitted for clarity) to illustrate the flat and rigid boronate ester based backbone.

motif, which has recently been used as a new acceptor in donor−acceptor conjugated polymers. This electron deficient dye can lead to intriguing properties such as broadband light absorption, high open circuit voltage and high mobilities and can reach relatively high power conversion efficiencies when implemented in organic photovoltaic devices.[19−22] The isoindigo dye has also been successfully implemented in COFs.[19,23] Furthermore, isoindigo building blocks can be used to obtain broad optical absorption from the visible into the near infrared region (NIR).[23]

Whereas highly symmetric dyes as for example the porphyrins or phthalocyanines discussed above have been successfully implemented into COFs, the incorporation of dyes with sterically demanding side chains or "kinked" (less symmetric) molecules into the backbone of 2D COFs is still a major challenge. Recently, we reported the template free microtubular self assembly of a COF based on imine condensation between tetrakis(4 aminophenyl)porphyrin (**TAPP**) and a diketopyrrolopyrrole (**DPP**) dialdehyde derivative.[24] In that report, the formation of a network containing strongly absorbing dyes and sterically demanding building blocks was demonstrated. **DPP TAPP COF** features remarkable optical absorption across the whole visible spectrum. Similar to the isoindigo building block, the **DPP** moiety is well studied in organic semiconducting polymers and small molecule based solar devices, showing high ambipolar carrier mobilities of around 0.3 $cm^2\ V^{-1}\ s^{-1}$ in organic field effect transistors[25−28] and high power conversion efficiencies.[29] To further extend the accessible family of **DPP** based COFs, we chose the alternative planar boronate ester coupling motif, allowing us to explore the photophysical properties of the **DPP** building block within a well defined molecular stack in an ordered porous structure.

Accordingly, here we report the synthesis of a novel COF based on **DPP** building blocks.[30,31] The framework synthesis is based on the formation of boronate ester groups via co condensation reaction of the new precursor ((2,5 bis(2 ethylhexyl) 3,6 dioxo 2,3,5,6 tetrahydropyrrolo[3,4 *c*] pyrrole 1,4 diyl)bis(thiophene 5,2 diyl))diboronic acid (**DPP2**) and commercially available hexahydroxytriphenylene (**HHTP**) (see Figure 1a). The **DPP2 HHTP COF** exhibits open pores with a high surface area, high crystallinity, and promising optical properties through framework induced stacking.

The **DPP2** linker was obtained in a 3 step synthesis described in the Supporting Information, whereas the **HHTP** counterpart is commercially available and was used without further purification. Subsequently, the synthesis conditions for **DPP2 HHTP COF** were screened with regard to solvents, solvent ratio, concentration, and reagent ratio (for more details, see the Supporting Information). All COF syntheses were carried out under solvothermal conditions in a 10 mL Schott Duran glass vial covered with a Teflon cap. In an optimized procedure, the organic precursors were dissolved in a solvent mixture of mesitylene and dioxane (1:1) and heated


DOI: 10.1021/acs.chemmater.8b02882
*Chem. Mater.* 2019, 31, 2707−2712

up to 100 °C for 24 h. A high concentration of the reagents turned out to be crucial for the formation of a highly ordered crystalline framework. After work up, including washing the crude product with dry acetone, **DPP2 HHTP COF** was obtained as a dark purple powder.

The powder X ray diffraction (PXRD) pattern of **DPP2 HHTP COF** is shown in Figure 1b. The XRD pattern indicates the formation of a highly crystalline framework with Bragg reflections centered at low 2$\theta$ values of 2.33, 4.13, 4.76, and 6.23°. These reflections are attributed to the 100, 110, 200, and 310 planes, respectively. Based on the symmetry of the applied building blocks including the sterically demanding alkyl groups pointing into the pores, the expected nearly hexagonal pore system with an eclipsed AA stacked layer model with planar boronate ester based backbone (Figure 1c) was simulated in the *P*1 and *P6/mcc* space groups using the Materials Studio software. The simulated diffraction pattern in the *P*1 space group provides a better description of our **DPP2 HHTP COF** (see Figure 1b and the Supporting Information). The final unit cell parameters in *P*1 were obtained by performing Pawley refinement and correspond to $a$ = 43.82 Å, $b$ = 44.57 Å, $c$ = 3.48 Å, $\alpha$ = 89.79°, $\beta$ = 89.53°, and $\gamma$ = 122.76° ($R_{wp}$ = 3.36% and $R_p$ = 2.52%).

To assess the porosity of **DPP2 HHTP COF**, nitrogen sorption measurements were carried out (Figure 2). Prior to the sorption experiments, the COF powder was degassed by keeping it at 150 °C in high vacuum overnight. The **DPP2 HHTP COF** features a type VI isotherm, typical for a well defined mesoporous framework structure, with a steep nitrogen uptake at about $p/p_0$ = 0.25, indicating mesopore filling. The Brunauer–Emmett–Teller (BET) surface area was calculated to be just above 1000 $m^2\ g^{-1}$ (adsorption branch in the range of $p/p_0$ = 0.07–0.21). Calculation of the COF pore size distribution reveals a maximum at 3.3 nm, which is in good agreement with the expected open pore system of the framework.

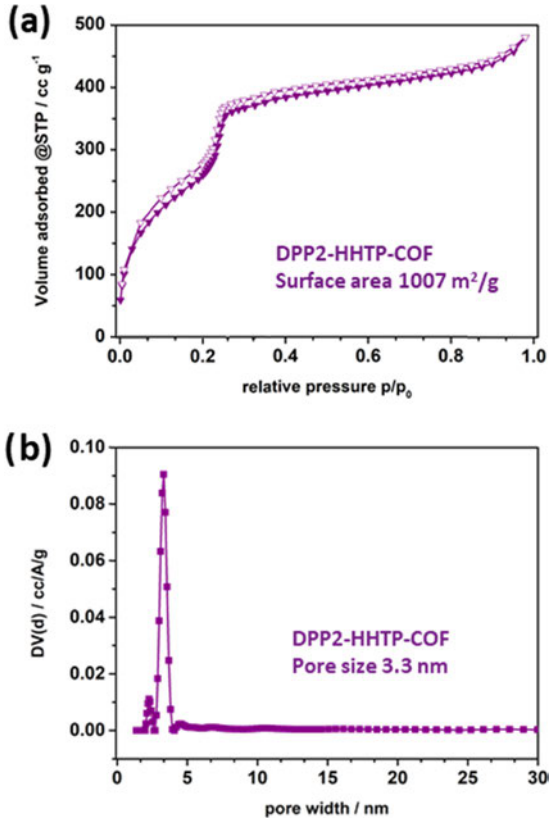


**Figure 2.** (a) Sorption isotherm (full symbol: adsorption; empty symbol: desorption) of **DPP2 HHTP COF** with calculated BET surface area and (b) pore size distribution of **DPP2 HHTP COF** with a calculated pore size of 3.3 nm.

Thermogravimetric analysis (TGA) revealed a framework thermal stability under dynamic conditions of up to 350 °C. At higher temperatures, this is followed by a weight loss of around 20%, which can most likely be attributed to the loss of the solubilizing alkyl side chains, and final framework decom position at 450 °C (see the Supporting Information).

Scanning electron microscopy (SEM) revealed that **DPP2 HHTP COF** predominantly adopts an intergrown needle like morphology, as shown in Figure 3a. In addition, a transmission electron microscopy (TEM) image of the framework illustrates crystalline COF domains that are highly intergrown and assemble in larger agglomerates (see Figure 3b).

In contrast to the recently reported imine based **DPP TAPP COF**, which exhibits a relatively flexible backbone where the imine bonds can rotate out of plane to accom modate the sterically demanding side chains,[24] our simulations for the PXRD data of **DPP2 HHTP COF** suggest that the boronate ester linkages in **DPP2 HHTP COF** enforce the formation of a planar backbone (see Figure 1c). This framework layout should be beneficial for promoting stacking interactions between the **DPP** molecules in the COF, thus leading to the enhanced crystallinity observed in the case of **DPP2 HHTP COF**. Based on molecular interactions, it is likely that the planar layers are stacked in a slightly slipped fashion, accounting for the sterically demanding side chains.[32] Whereas Dichtel et al. implemented a thienoisoindigo derivative to form a kinked imine based COF,[19] here we report the successful formation of a boronate based crystalline framework with even larger, sterically demanding ethylhexyl groups, harnessing the favorable stacking of the **DPP** cores to form a well defined kinked COF structure.

The optical characterization of bulk powder samples of **DPP2 HHTP COF** is summarized in Figure 4. As mentioned above, this COF features a dark purple color with a broad optical absorption ranging from the UV up to almost 700 nm (Figure 4a), as determined by diffuse reflectance measure ments. The photoluminescence (PL) exhibits two distinct emission peaks, at around 620 and 680 nm, and covers a broad spectral range from the visible to the near infrared (Figure 4a). A time correlated single photon counting (TCSPC) measure ment of the peak emission at 620 nm is shown in Figure 4b, and the longest lifetime is fitted with around 5.6 ns.[33] We note, however, that the overall contribution of this decay component is small (3%) and the faster decay channels of 0.19 ns (61%) and 0.62 ns (36%) are predominant. The origin of the decay pathways cannot be determined through the TCSPC measure ment and will not be further elucidated in this study. The decay at 680 nm shows very similar timescales, and a homogeneous decay across the whole spectrum can be observed in the time resolved emission spectra (TRES) scan (see the Supporting Information, Figure S11). The UV–vis studies of a **DPP2** film (see the Supporting Information, Section S8.1) reveal a red shifted absorption as compared to monomers in solution. We attribute this red shift to the formation of well defined stacks with J type interaction along the COF molecular column.[34–36] This is further supported by


DOI: 10.1021/acs.chemmater.8b02882
*Chem. Mater.* 2019, 31, 2707–2712

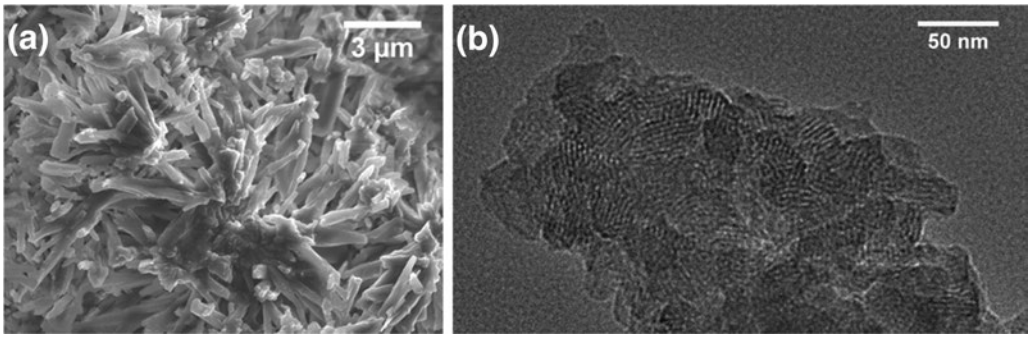


**Figure 3.** (a) SEM image of **DPP2 HHTP COF** showing needle like agglomerate morphology and (b) TEM image illustrating the intergrown COF crystallites exhibiting small domain sizes.

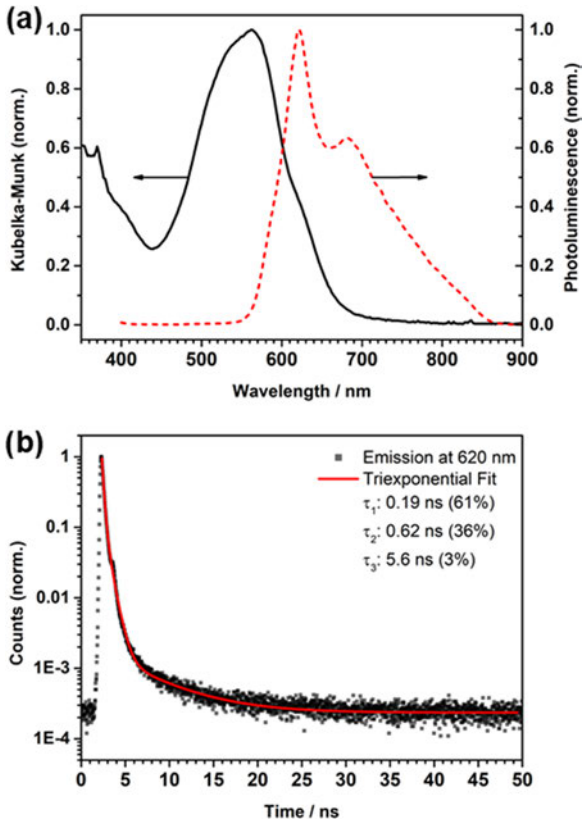


**Figure 4.** (a) Absorption (black, solid) and photoluminescence (red, dashed) spectra of the **DPP2 HHTP COF**. Absorption was measured through diffuse reflectance measurements and converted using the Kubelka–Munk equation. (b) Time correlated single photon count ing (TCSPC) histogram (black squares), corresponding triexponen tial fit (solid line, red), and the respective fitted lifetimes. The percentages given with the different lifetimes correspond to the respective contribution to the overall decay intensity.

the observed intensity sequence of the absorption peaks, with no oscillator strength gained by the second peak, which would be characteristic for classical H aggregates.[37] We note that due to the slightly slipped stacking of the **DPP2 HHTP** sheets, the stack is not a J aggregate in the classical Kasha picture but rather a molecular arrangement showing a strong J type character, which might be induced by CT interactions.[36] A comparison of the PL emission spectra of the crystalline and amorphous **DPP2 HHTP COF** with the individual **DPP2** and **HHTP** precursors indicates that the main emission at around 620 nm can be attributed to a **DPP2** aggregate with J type interaction, as in the case for neat solid **DPP2**, whereas the broad peak up to over 850 nm seems to originate from transitions generated through the COF formation (see the Supporting Information, Section S8). Furthermore, PXRD measurements confirm the existence of a crystalline framework without the residues of the precursors, hence the precursors are not expected to contribute to the optical spectra (see the Supporting Information, Section S9). More information on the optical measurements, instrument response, fitting, and the full set of lifetimes with their respective fitting uncertainties can be found in the Supporting Information (Section S8).

The conductivity of **DPP2 HHTP COF** was determined on a compressed powder pellet, using a four point probe, also called the van der Pauw measurement technique. In these measurements, based on the Hall effect, several material parameters can be determined, ultimately yielding the electric conductivity, which is an intriguing parameter to evaluate with regards to the well aligned photoactive dyes. The as synthesized bulk material was finely grounded manually and pressed into a pellet with 10 mm diameter by applying different pressures. During this procedure, the fundamental characteristics of the **DPP2 HHTP COF** structure (mainly crystallinity) could be preserved and structural changes could not be detected by PXRD (see the Supporting Information, Section S6). Moreover, several batches of the **DPP2 HHTP COF** pressed pellets were measured to get a representative averaged electrical conductivity value. For the crystalline **DPP2 HHTP COF**, we measured conductivities of up to 2.2 $\times$ $10^{-6}$ S $cm^{-1}$ (for more details, see Supporting Information, Section S7). This is an order of magnitude higher than reports for other boronate ester based COFs in the literature.[38]

To evaluate the impact of crystallinity on the electrical conductivity, van der Pauw measurements were performed and the electrical conductivity was determined for amorphous **DPP2 HHTP COF** powder. For this purpose, **DPP2** and **HHTP** were allowed to react under reaction conditions yielding an amorphous polymer by changing solvents and reaction time (see the Supporting Information, Section S4). The samples exhibited conductivities of around 2 $\times$ $10^{-7}$ S $cm^{-1}$, one order of magnitude smaller than the peak value for the crystalline pellets (but showing less variation across different samples).

A comparison of the values obtained for the crystalline and amorphous pellets indicates that the conductivity of the material is limited by several parameters. Grain boundaries between different domains in the crystalline COF would be expected to represent barriers for conductivity. Hence, the bulk conductivity will depend on the orientation and number of


DOI: 10.1021/acs.chemmater.8b02882
Chem. Mater. 2019, 31, 2707–2712

grain boundaries in the current path. In the van der Pauw geometry, conductivity is measured within the pellet plane. In the DPP2 HHTP COF, charge transport most likely occurs along the molecular stacks and the largest conductivity is measured at $2.2 \times 10^{-6}$ S cm$^{-1}$. Here, the overall measurement strongly depends on the spontaneous organization of the single crystallites between the contacts, which leads to the significant difference in conductivity values (see the Supporting Information, Table S5). In the case of crystallites being oriented with their COF stacking axis along the electrical conduction channel, conductivity is much higher than in the case where their stacking direction is perpendicular to the direct line between the contacts, leading to reduced transport and values of around $10^{-8}$ S cm$^{-1}$. In contrast, in the amorphous powder, there is no preferential direction of charge transport. Therefore, the overall measurement path across different domains in the crystalline COF can be compared to a homogeneous conduction channel in the amorphous material. This results in very similar values of around $10^{-7}$ S cm$^{-1}$ across different samples of the latter (see the Supporting Information, Table S6), which are generally smaller than the peak values achieved in crystalline samples. The conductivity of the neat precursor molecular building blocks (prepared as pellets and measured as described above, ca. $1 \times 10^{-8}$ S cm$^{-1}$) was significantly below the peak value of the condensed network of the corresponding DPP2 HHTP COF. This finding underscores the importance of assembling the building blocks in a $\pi$ stacked framework and its orientation to achieve substantial conductivity (see the Supporting Information, Section S7).

In this study, we have demonstrated the successful implementation of DPP chromophores and HHTP into a boronate ester linked COF exhibiting a highly porous and crystalline structure. We attribute this to the rather rigid and planar boronate ester bond, inducing favorable stacking interactions between the adjacent COF layers. Even rather short reaction times result in a highly crystalline framework with a strong absorption across the visible spectrum. The longest singlet lifetime component of 5.6 ns is attributed to the high crystallinity and efficient electronic coupling of the 2D COF layers, resulting in efficient stabilization of the excitons across the DPP stacks.

Furthermore, this is the first report on macroscopic conductivity values for boronate ester based framework powders, obtained with four point probe Hall measurements. While maintaining the structural characteristics of the material, we were able to produce pellets of the bulk material that showed conductivities of up to $2.2 \times 10^{-6}$ S cm$^{-1}$, being the highest value for boronate ester based COF bulk materials reported to date. The spectroscopic data together with the relatively high conductivity values hold promise for DPP2 HHTP COF and related COFs concerning future applications in solar cells or as conductive layers, e.g., in transistor devices.

## ■ ASSOCIATED CONTENT

### ● Supporting Information

The Supporting Information is available free of charge on the ACS Publications website at DOI: 10.1021/acs.chemmater.8b02882.

Structural characterization, synthetic procedures, conductivity measurements, IR, PXRD, TGA, PL spectra, TCSPC, TRES spectra, details for J type interactions (PDF)

## ■ AUTHOR INFORMATION


### Corresponding Authors

*E mail: dana.medina@cup.uni muenchen.de (D.D.M.).
*E mail: bein@lmu.de (T.B.).

### ORCID

Sabrina Rager: 0000 0002 3938 1790
Andreas C. Jakowetz: 0000 0001 7804 7210
Bappaditya Gole: 0000 0002 0001 6569
Florian Beuerle: 0000 0001 7239 8327
Dana D. Medina: 0000 0003 4759 8612
Thomas Bein: 0000 0001 7248 5906


### Author Contributions

The manuscript was written through contributions of all authors. All authors have given approval to the final version of the manuscript.

### Notes

The authors declare no competing financial interest.

## ■ ACKNOWLEDGMENTS

The authors are grateful for funding from the German Science Foundation (DFG, Research Cluster Nanosystems Initiative Munich (NIM)) and the Research Network "Solar Technologies go Hybrid" (Free State of Bavaria). The research leading to these results has received funding from the European Research Council under the European Union's Seventh Framework Programme (FP7/2007 2013)/ERC grant agreement no. 321339. We thank Dr. Steffen Schmidt for scanning electron microscopy and for transmission electron microscopy.

## ■ REFERENCES


(1) Côté, A. P.; Benin, A. I.; Ockwig, N. W.; O'Keeffe, M.; Matzger, A. J.; Yaghi, O. M. Porous, Crystalline, Covalent Organic Frameworks. *Science* **2005**, *310*, 1166−1170.

(2) Uribe Romo, F. J.; Hunt, J. R.; Furukawa, H.; Klöck, C.; O'Keeffe, M.; Yaghi, O. M. A Crystalline Imine Linked 3 D Porous Covalent Organic Framework. *J. Am. Chem. Soc.* **2009**, *131*, 4570−4571.

(3) Lohse, M. S.; Bein, T. Covalent Organic Frameworks: Structures, Synthesis, and Applications. *Adv. Funct. Mater.* **2018**, *28*, No. 1705553.

(4) Beuerle, F.; Gole, B. Covalent Organic Frameworks and Cage Compounds: Design and Applications of Polymeric and Discrete Organic Scaffolds. *Angew. Chem., Int. Ed.* **2018**, *57*, 4850−4878.

(5) Keller, N.; Bessinger, D.; Reuter, S.; Calik, M.; Ascherl, L.; Hanusch, F. C.; Auras, F.; Bein, T. Oligothiophene Bridged Conjugated Covalent Organic Frameworks. *J. Am. Chem. Soc.* **2017**, *139*, 8194−8199.

(6) Calik, M.; Auras, F.; Salonen, L. M.; Bader, K.; Grill, I.; Handloser, M.; Medina, D. D.; Dogru, M.; Löbermann, F.; Trauner, D.; Hartschuh, A.; Bein, T. Extraction of Photogenerated Electrons and Holes from a Covalent Organic Framework Integrated Heterojunction. *J. Am. Chem. Soc.* **2014**, *136*, 17802−17807.

(7) Medina, D. D.; Sick, T.; Bein, T. Photoactive and Conducting Covalent Organic Frameworks. *Adv. Energy Mater.* **2017**, *7*, No. 1700387.

(8) Medina, D. D.; Petrus, M. L.; Jumabekov, A. N.; Margraf, J. T.; Weinberger, S.; Rotter, J. M.; Clark, T.; Bein, T. Directional Charge Carrier Transport in Oriented Benzodithiophene Covalent Organic Framework Thin Films. *ACS Nano* **2017**, *11*, 2706−2713.

(9) Mulzer, C. R.; Shen, L.; Bisbey, R. P.; McKone, J. R.; Zhang, N.; Abruña, H. D.; Dichtel, W. R. Superior Charge Storage and Power Density of a Conducting Polymer Modified Covalent Organic Framework. *ACS Cent. Sci.* **2016**, *2*, 667−673.




DOI: 10.1021/acs.chemmater.8b02882
*Chem. Mater.* 2019, 31, 2707−2712

(10) Ding, H.; Li, Y.; Hu, H.; Sun, Y.; Wang, J.; Wang, C.; Wang, C.; Zhang, G.; Wang, B.; Xu, W.; Zhang, D. A Tetrathiafulvalene Based Electroactive Covalent Organic Framework. *Chem. Eur. J.* **2014**, *20*, 14614−14618.
(11) Liao, H.; Wang, H.; Ding, H.; Meng, X.; Xu, H.; Wang, B.; Ai, X.; Wang, C. A 2D porous porphyrin based covalent organic framework for sulfur storage in lithium sulfur batteries. *J. Mater. Chem. A* **2016**, *4*, 7416−7421.
(12) Jin, S.; Supur, M.; Addicoat, M.; Furukawa, K.; Chen, L.; Nakamura, T.; Fukuzumi, S.; Irle, S.; Jiang, D. Creation of Superheterojunction Polymers via Direct Polycondensation: Segregated and Bicontinuous Donor−Acceptor π Columnar Arrays in Covalent Organic Frameworks for Long Lived Charge Separation. *J. Am. Chem. Soc.* **2015**, *137*, 7817−7827.
(13) Lin, G.; Ding, H.; Chen, R.; Peng, Z.; Wang, B.; Wang, C. 3D Porphyrin Based Covalent Organic Frameworks. *J. Am. Chem. Soc.* **2017**, *139*, 8705−8709.
(14) Hou, Y.; Zhang, X.; Wang, C.; Qi, D.; Gu, Y.; Wang, Z.; Jiang, J. Novel imine linked porphyrin covalent organic frameworks with good adsorption removing properties of RhB. *New J. Chem.* **2017**, *41*, 6145−6151.
(15) Spitler, E. L.; Dichtel, W. R. Lewis acid catalysed formation of two dimensional phthalocyanine covalent organic frameworks. *Nat. Chem.* **2010**, *2*, 672.
(16) Ding, X.; Guo, J.; Feng, X.; Honsho, Y.; Guo, J.; Seki, S.; Maitarad, P.; Saeki, A.; Nagase, S.; Jiang, D. Synthesis of Metallophthalocyanine Covalent Organic Frameworks That Exhibit High Carrier Mobility and Photoconductivity. *Angew. Chem., Int. Ed.* **2011**, *50*, 1289−1293.
(17) Spitler, E. L.; Colson, J. W.; Uribe Romo, F. J.; Woll, A. R.; Giovino, M. R.; Saldivar, A.; Dichtel, W. R. Lattice Expansion of Highly Oriented 2D Phthalocyanine Covalent Organic Framework Films. *Angew. Chem., Int. Ed.* **2012**, *51*, 2623−2627.
(18) Neti, V. S. P. K.; Wu, X.; Hosseini, M.; Bernal, R. A.; Deng, S.; Echegoyen, L. Synthesis of a phthalocyanine 2D covalent organic framework. *CrystEngComm* **2013**, *15*, 7157−7160.
(19) Matsumoto, M.; Dasari, R. R.; Ji, W.; Feriante, C. H.; Parker, T. C.; Marder, S. R.; Dichtel, W. R. Rapid, Low Temperature Formation of Imine Linked Covalent Organic Frameworks Catalyzed by Metal Triflates. *J. Am. Chem. Soc.* **2017**, *139*, 4999−5002.
(20) Lei, T.; Wang, J. Y.; Pei, J. Design, Synthesis, and Structure−Property Relationships of Isoindigo Based Conjugated Polymers. *Acc. Chem. Res.* **2014**, *47*, 1117−1126.
(21) Wang, E.; Mammo, W.; Andersson, M. R. 25th Anniversary Article: Isoindigo Based Polymers and Small Molecules for Bulk Heterojunction Solar Cells and Field Effect Transistors. *Adv. Mater.* **2014**, *26*, 1801−1826.
(22) Deng, Y.; Liu, J.; Wang, J.; Liu, L.; Li, W.; Tian, H.; Zhang, X.; Xie, Z.; Geng, Y.; Wang, F. Dithienocarbazole and Isoindigo based Amorphous Low Bandgap Conjugated Polymers for Efficient Polymer Solar Cells. *Adv. Mater.* **2014**, *26*, 471−476.
(23) Bessinger, D.; Ascherl, L.; Auras, F.; Bein, T. Spectrally Switchable Photodetection with Near Infrared Absorbing Covalent Organic Frameworks. *J. Am. Chem. Soc.* **2017**, *139*, 12035−12042.
(24) Gole, B.; Stepanenko, V.; Rager, S.; Grüne, M.; Medina, D. D.; Bein, T.; Würthner, F.; Beuerle, F. Microtubular Self Assembly of Covalent Organic Frameworks. *Angew. Chem., Int. Ed.* **2018**, *57*, 846−850.
(25) Zhao, B.; Sun, K.; Xue, F.; Ouyang, J. Isomers of dialkyl diketo pyrrolo pyrrole: Electron deficient units for organic semiconductors. *Org. Electron.* **2012**, *13*, 2516−2524.
(26) Li, W.; Hendriks, K. H.; Wienk, M. M.; Janssen, R. A. J. Diketopyrrolopyrrole Polymers for Organic Solar Cells. *Acc. Chem. Res.* **2016**, *49*, 78−85.
(27) Di Pietro, R.; Erdmann, T.; Carpenter, J. H.; Wang, N.; Shivhare, R. R.; Formanek, P.; Heintze, C.; Voit, B.; Neher, D.; Ade, H.; Kiriy, A. Synthesis of High Crystallinity DPP Polymers with Balanced Electron and Hole Mobility. *Chem. Mater.* **2017**, *29*, 10220−10232.
(28) Głowacki, E. D.; Coskun, H.; Blood Forsythe, M. A.; Monkowius, U.; Leonat, L.; Grzybowski, M.; Gryko, D.; White, M. S.; Aspuru Guzik, A.; Sariciftci, N. S. Hydrogen bonded diketopyrro lopyrrole (DPP) pigments as organic semiconductors. *Org. Electron.* **2014**, *15*, 3521−3528.
(29) Li, Y.; Sonar, P.; Murphy, L.; Hong, W. High mobility diketopyrrolopyrrole (DPP) based organic semiconductor materials for organic thin film transistors and photovoltaics. *Energy Environ. Sci.* **2013**, *6*, 1684−1710.
(30) Grzybowski, M.; Gryko, D. T. Diketopyrrolopyrroles: Synthesis, Reactivity, and Optical Properties. *Adv. Opt. Mater.* **2015**, *3*, 280−320.
(31) Kaur, M.; Choi, D. H. Diketopyrrolopyrrole: brilliant red pigment dye based fluorescent probes and their applications. *Chem. Soc. Rev.* **2015**, *44*, 58−77.
(32) Lohse, M. S.; Rotter, J. M.; Margraf, J. T.; Werner, V.; Becker, M.; Herbert, S.; Knochel, P.; Clark, T.; Bein, T.; Medina, D. D. From benzodithiophene to diethoxy benzodithiophene covalent organic frameworks structural investigations. *CrystEngComm* **2016**, *18*, 4295−4302.
(33) Jin, S.; Furukawa, K.; Addicoat, M.; Chen, L.; Takahashi, S.; Irle, S.; Nakamura, T.; Jiang, D. Large pore donor acceptor covalent organic frameworks. *Chem. Sci.* **2013**, *4*, 4505−4511.
(34) Kaiser, T. E.; Wang, H.; Stepanenko, V.; Würthner, F. Supramolecular Construction of Fluorescent J Aggregates Based on Hydrogen Bonded Perylene Dyes. *Angew. Chem., Int. Ed.* **2007**, *46*, 5541−5544.
(35) Würthner, F.; Kaiser, T. E.; Saha Möller, C. R. J Aggregates: From Serendipitous Discovery to Supramolecular Engineering of Functional Dye Materials. *Angew. Chem., Int. Ed.* **2011**, *50*, 3376−3410.
(36) Hestand, N. J.; Spano, F. C. Molecular Aggregate Photophysics beyond the Kasha Model: Novel Design Principles for Organic Materials. *Acc. Chem. Res.* **2017**, *50*, 341−350.
(37) Spano, F. C. The Spectral Signatures of Frenkel Polarons in H and J Aggregates. *Acc. Chem. Res.* **2010**, *43*, 429−439.
(38) Duhović, S.; Dincă, M. Synthesis and Electrical Properties of Covalent Organic Frameworks with Heavy Chalcogens. *Chem. Mater.* **2015**, *27*, 5487−5490.


DOI: 10.1021/acs.chemmater.8b02882
*Chem. Mater.* 2019, 31, 2707−2712